




Improved Sensitivity of Ultrasound-Based Subharmonic Aided Pressure Estimation Using Monodisperse Microbubbles

Wim van Hove, PhD, Miguel de Vargas Serrano, MSc, Lisa te Winkel, BSc, Flemming Forsberg, PhD , Jaydev K. Dave, PhD, Kausik Sarkar, PhD , Corinne E. Wessner, MBA, John R. Eisenbrey, PhD 

Received August 31, 2021, from the Solstice Pharmaceuticals B.V, Enschede, Netherlands (W.v.H., M.d.V.S., L.t.W.); Department of Radiology, Thomas Jefferson University, Philadelphia, PA, USA (F.F., J.K.D., C.E.W., J.R.E.); and Department of Mechanical and Aerospace Engineering, The George Washington University, Washington, DC, USA (K.S.). Manuscript accepted for publication October 1, 2021.

Funding for this work was provided in part by the National Institutes of Health under the National Institute of Diabetes and Digestive and Kidney Diseases grant DK118964.

WVH: Managing Director of Solstice Pharmaceuticals. MDVS: Employee of Solstice Pharmaceuticals. LTW: Employee of Solstice Pharmaceuticals. FF: Equipment, contrast agent, and grants support from GE Healthcare. Equipment and grant support from Canon Medical Systems America. Equipment and grant support from the Butterfly Network. Drug support and speaker honorarium from Lantheus Medical Imaging. Equipment support from Siemens Healthineers. Drug support from Bracco. Consultant for Samumed and Exact Therapeutics. JKD: Contrast agent support from Lantheus Medical Imaging and GE Healthcare. Research grant from Philips. KS: None. CEW: Consulting; Bracco Imaging. JRE: Equipment, contrast agent, and grants support from GE Healthcare. Drug support and speaker honorarium from Lantheus Medical Imaging. Equipment support from Siemens Healthineers. Royalties from Elsevier.

Address correspondence to John R. Eisenbrey, PhD, Department of Radiology, Thomas Jefferson University, 132 South 10th St., Philadelphia, PA 19107, USA,

E-mail: john.eisenbrey@jefferson.edu

Abbreviations

GSD, geometric standard deviations; PDI, polydispersity index; SHAPE, subharmonic aided pressure estimation; UCAs, ultrasound contrast agents

doi:10.1002/jum.15861

Objectives—Subharmonic aided pressure estimation (SHAPE) has been shown effective for noninvasively measuring hydrostatic fluid pressures in a variety of clinical applications. The objective of this study was to explore potential improvements in SHAPE sensitivity using monodisperse microbubbles.

Methods—Populations of monodisperse microbubbles were created using a commercially available microfluidics device (Solstice Pharmaceuticals). Size distributions were assessed using a Coulter Counter and stability of the distribution following fabrication was evaluated over 24 hours. Attenuation of the microbubble populations from 1 to 10 MHz was then quantified using single element transducers to identify each formulation's resonance frequency. Frequency spectra over increasing driving amplitudes were investigated to determine the nonlinear phases of subharmonic signal generation. SHAPE sensitivity was evaluated in a hydrostatic pressure-controlled water bath using a Logiq E10 scanner (GE Healthcare).

Results—Monodisperse lipid microbubble suspensions ranging from 2.4 to 5.3 μm in diameter were successfully created and they showed no discernable change in size distribution over 24 hours following activation. Calculated resonance frequencies ranged from 2.1 to 6.3 MHz and showed excellent correlation with microbubble diameter ($R^2 > 0.99$). When investigating microbubble frequency response, subharmonic signal occurrence was shown to begin at 150 kPa peak negative pressure, grow up to 225 kPa, and saturate at approximately 250 kPa. Using the Logiq E10, monodisperse bubbles demonstrated a SHAPE sensitivity of -0.17 dB/mmHg , which was nearly twice the sensitivity of the commercial polydisperse microbubble currently being used in clinical trials.

Conclusions—Monodisperse microbubbles have the potential to greatly improve the sensitivity of SHAPE for the noninvasive measurement of hydrostatic pressures.

Key Words—microfluidics; monodisperse; pressure estimation; subharmonic; ultrasound contrast agents

Hydrostatic pressure measurements are required for the diagnosis and management of a wide variety of clinical diseases.^{1–3} Currently, absolute pressure measurements are obtained by the invasive placement of pressure sensing catheters, with the patient under partial or full anesthesia. While these techniques are well established, the controversy regarding

the possibility of increased mortality and utilization of resources associated with pressure catheter use has highlighted the need for accurate noninvasive measurement of fluid pressures in several applications.^{1–3} In addition, the costs and associated risks of these procedures (primarily attributed to the need for anesthesia) limit the regularity of data collection via catheter.

Ultrasound contrast agents (UCAs) have been proposed as a tool for noninvasive quantification of fluid pressure. A number of microbubble-based pressure estimation techniques have been proposed, the majority of which rely on the shift in bubble resonance frequency as a function of pressure.^{4–6} However, these methods are limited by their lack of sensitivity to measure small pressure variations and produced *in vitro* errors exceeding 30% or as high as 50 mmHg, which is clinically unacceptable.⁷

As an alternative, the amplitude of a microbubble at the subharmonic frequency (half the transmit frequency) varies with hydrostatic pressure.⁸ As a function of incident acoustic pressure, the subharmonic signals undergo three stages: occurrence, growth, and saturation.⁸ In the growth stage, the subharmonic component rapidly increases with incident acoustic pressure and usually has high amplitudes above the background noise (or occurrence stage). Within this regime, the subharmonic amplitude shows an inverse and linear relationship with the surrounding fluid pressure for most commercial UCAs.^{8,9} This phenomenon has led to the development and refinement of subharmonic aided pressure estimation (SHAPE). Using clinically approved UCAs, this approach has been shown to provide accurate *in vivo* pressure estimates in a variety of animal models.^{10–12} More recently, the utility of SHAPE has been validated in clinical trials for the diagnosis of portal hypertension,^{13–15} quantifying cardiac pressures,¹⁶ and monitoring interstitial fluid pressures in tumors over the course of neoadjuvant chemotherapy.¹⁷

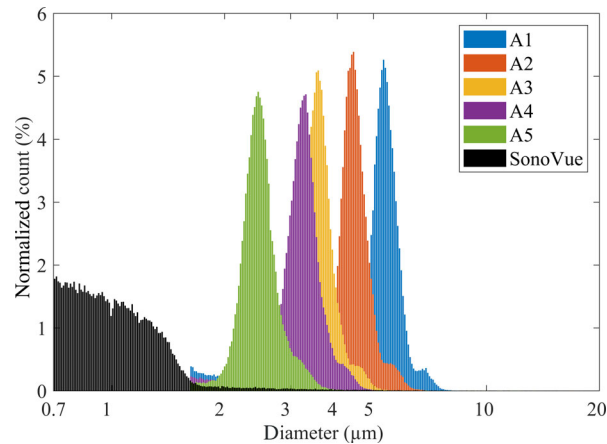
The SHAPE algorithm is now implemented on two commercial ultrasound scanners for general use.¹⁸ However, its sensitivity at lower hydrostatic pressures is still suboptimal. Currently, SHAPE provides up to 14 dB reduction in the subharmonic amplitude over a pressure increase of 180 mmHg (ie, 0.078 dB/mmHg) under optimized acoustic conditions.⁹ However, our group and others have developed theoretical models of the SHAPE response based on individual bubbles and identified potential sensitivities of >0.13 dB/mmHg using optimized microbubble parameters.^{19–23} Thus, the potential

exists to triple the current sensitivity of SHAPE, thereby greatly reducing the overall errors associated with lower pressure measurements. However, these models assume a single microbubble or a monodisperse bubble population, which does not reflect the current UCAs used in the clinic. One solution to this limitation has focused on advances in the field of microfluidics that have enabled fast and inexpensive fabrication of monodisperse stabilized microbubbles.^{24–26} These systems are now commercially available for research applications and provide customization of microbubble size and material properties. Consequently, the purpose of this study was to investigate the use of monodisperse microbubbles for SHAPE and ascertain their potential to improve its overall sensitivity.

Methods

This manuscript is exempted from obtaining informed consent. Institutional review board and institutional animal care and use committee approvals were not obtained for this study as only *in vitro* results were obtained. Monodisperse microbubbles were created using a commercial microfluidics device specifically designed for UCA fabrication (Microsphere Creator; Solstice Pharmaceuticals, Enschede, Netherlands). This system uses a cartridge of proprietary lipid mixture (primarily 1,2-dipalmitoyl-sn-glycero-3-phosphocholine and *N*-(carbonyl-methoxypolyethylene glycol-5000)-1,2-dipalmitoyl-sn-glycero-3-phosphoethanolamine) that is activated prior to use to create octoflouoropropane microbubbles with a lipid shell. During activation, the gas-to-liquid flow rate ratio in the microfluidic chip was tailored to the desired microbubble diameter. Following activation by gentle hand agitation for 30 seconds, the polydispersity index, mean bubble diameter, and geometric standard deviations (GSD) were measured using a Coulter Counter (MultiSizer 4e, Beckman Coulter, Brea, CA) and compared to SonoVue (Bracco Spa, Milan, Italy). The polydispersity index is a unitless measure defined as the square of the particle size standard deviation divided by the mean particle diameter, where a value of 0 represents a perfectly uniform sample and 1 represents a highly polydisperse sample. The geometric standard deviation is a dimensionless number and reflects how spread out a set of numbers is

Figure 1. Example data showing size distribution of SonoVue (black) ultrasound contrast agent and five monodisperse lipid microbubbles with varying diameters.



relative to the average geometric mean. Following activation, shelf-life stability was evaluated under room temperature conditions by repeating size measurements after 5 minutes, 3 hours, 6 hours, and 24 hours.

Resonance frequency of the varying monodisperse populations and SonoVue at ambient pressure was quantified using an attenuation approach described by de Jong et al.²⁷ Briefly, microbubbles were held in a container at room temperature with inner dimensions of $4 \times 4 \times 8$ cm ($W \times L \times H$) and continuously stirred in 110 ml of air-saturated saline. This chamber contains an acoustically transparent window with diameter of 2.8 cm in the front wall and a 1 cm metallic plate for reflecting the acoustic beam in the rear wall. The window membrane was 80- μ m thick polyester film (Sadipal Plus 80, Sadipal, Girona, Spain). A 5.0 MHz immersion transducer (V309-SU, Olympus, Waltham, MA) was used for transmitting a broad-band pulse at 2.5 Hz using a Pulser-Receiver (DPR300, JSR Ultrasonic, Pittsford, NY) in echo mode. Initial broadband pulses were generated and averaged over 50 pulses at 2.5 Hz to calculate the frequency response of the background. Then 7.5 μ l of monodisperse microbubbles were added to the container and homogeneously distributed through continuous stirring of the solution using a magnetic stir bar to obtain a number density of around 10,000 microbubbles per ml. A further 50 pulses were recorded and averaged to calculate the frequency response of the monodisperse microbubbles. Finally, the attenuation as a function of frequency was calculated by subtracting the background

Figure 2. Size distribution stability over 24 hours post activation of a 4 μ m bubble. Less than 10% change in mode diameter of the bubble is observed over this period (insert), indicating the bubble size distribution remains stable over time. The size distribution is represented as a volume-weighted size distribution normalized by area.

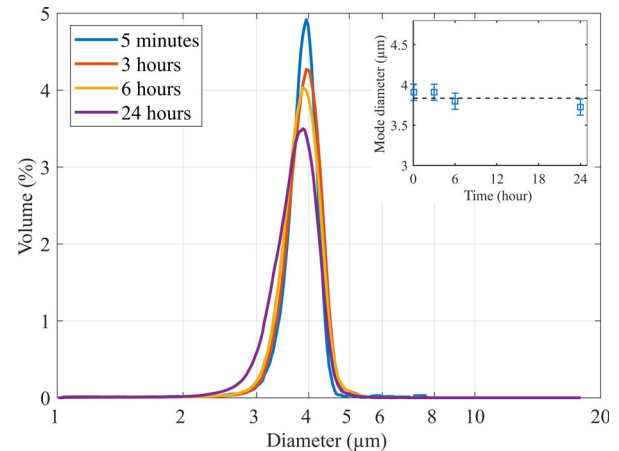
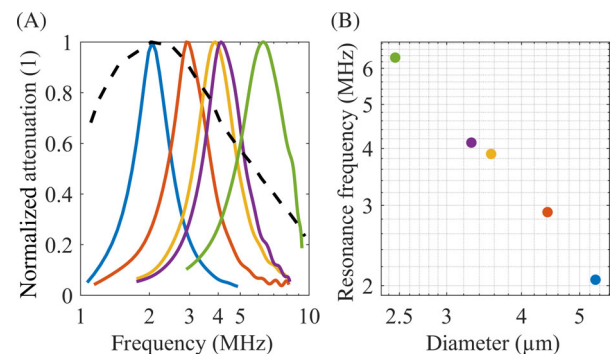


Figure 3. (A) Attenuation curves of the different microbubble populations identified in Figure 1 (black = SonoVue, Blue, orange, yellow, purple, and green = 2.4, 3.3, 3.6, 4.4, and 5.3 μ m diameter monodisperse microbubbles, respectively). (B) Correlation of resonance frequencies from the monodisperse bubble data on left with microbubble diameter ($R^2 > 0.99$).



signal from the bubble signal and normalizing it for the transducer transfer function.

The ability of monodisperse microbubbles to generate subharmonic signals was investigated in a room temperature water bath using single element transducers. For these experiments, 4 μ m bubbles were suspended and insonated at 3.6 MHz (the bubble's approximate resonance frequency). An arbitrary 64 cycle pulse train with rectangular window was generated and averaged over 50 pulses at 100 Hz. The frequency response was then calculated and plotted at

Figure 4. Frequency response of a 4 μm monodisperse bubble population insonated at a frequency of 3.6 MHz at ambient pressure. Subharmonic signal begins to occur at 150 kPa peak negative pressure, undergoes growth up to 225 kPa, and reaches the saturation phase at approximately 250 kPa. Plotting the relationship between subharmonic amplitude and acoustic pressure generates a nonlinear S-curve (bottom right) normally associated with SHAPE.

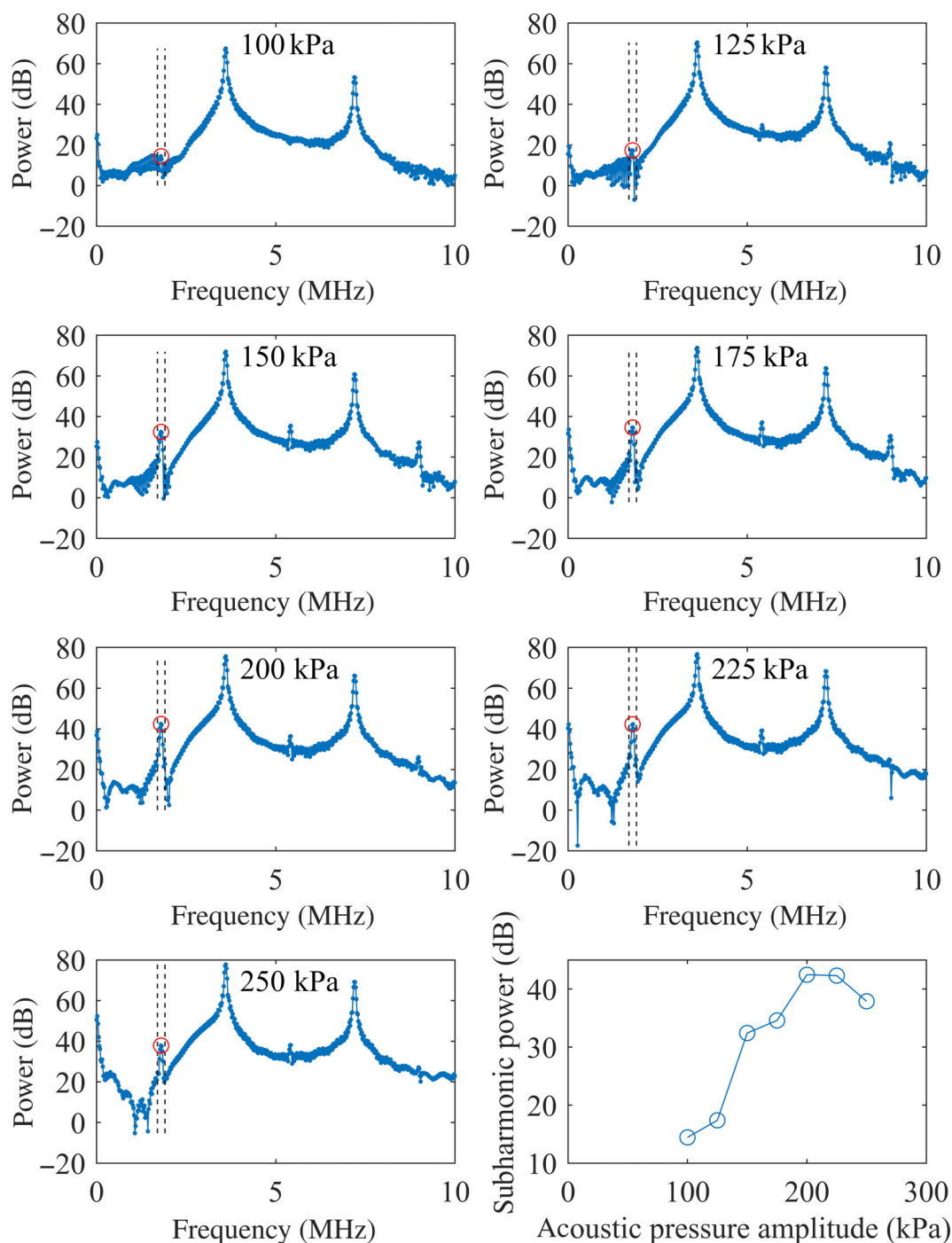
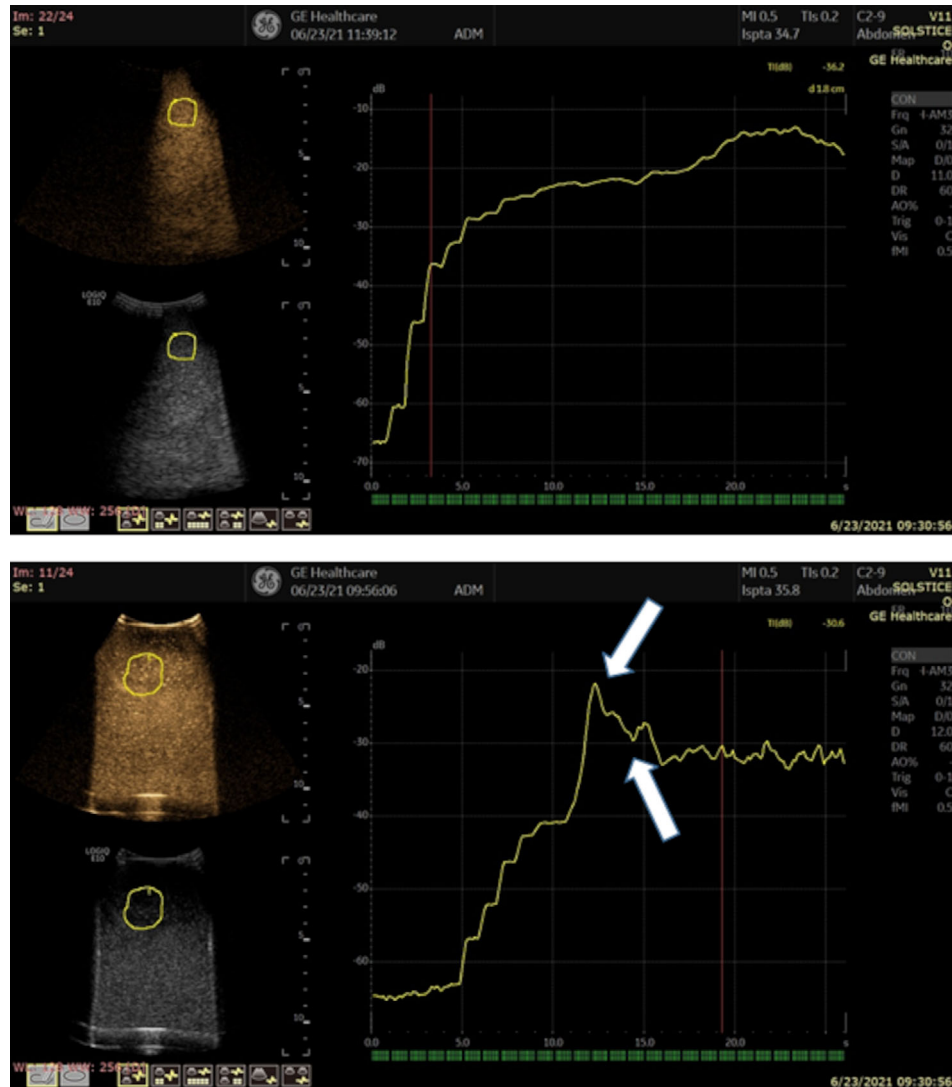


Figure 5. SHAPE power optimization process on the Logiq E10 for Sonazoid (top image) and 3.0 μm monodisperse microbubbles (bottom). In the left panels, both subharmonic (gold image) and B-mode (grayscale) enhancement is observed. In the right panels, signal intensity (y-axis) increases over time (x-axis) as the acoustic output is incrementally increased to a mechanical index of 0.5 at a fixed rate. Resultantly, this provides an indicator of subharmonic signal as a function of acoustic output power. A nonlinear S curve response is seen for both agents with subharmonic occurrence, growth, and saturation phases taking place. Microbubble destruction of the monodisperse agent is also seen at higher acoustic pressures, indicating bubble destruction (white arrows).

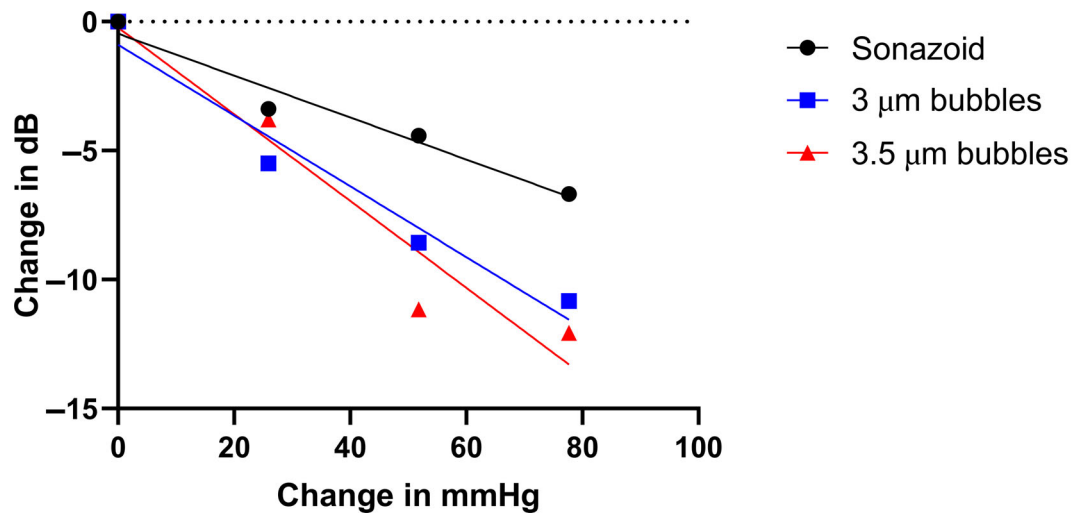


driving pressure amplitudes ranging from 100 to 250 kPa peak negative pressure.

Microbubble SHAPE sensitivity was also evaluated using commercially available software on the GE Logiq E10.¹⁸ Two monodisperse microbubble formulations consisting of 3.0 and 3.5 μm diameter bubbles were used as well as the commercial UCA Sonazoid (GE Healthcare, Oslo, Norway). Following manual agitation, 0.15 ml of

each microbubble solution was suspended in 600 ml of phosphate-buffered saline at room temperature. This resulted in a number density of approximately 51,000 microbubbles per ml for the 3.0 μm microbubbles and 40,000 microbubbles per ml for the 3.5 μm monodisperse microbubbles. The microbubble mixture was placed in a custom-built, acrylic pressurized tank with an acoustically transparent window and continuously stirred.⁹

Figure 6. Subharmonic response of Sonazoid (black), 3 μm monodisperse microbubbles (blue), and 3.5 μm monodisperse microbubbles (red) in response to increasing hydrostatic pressure.



Imaging was performed using a C2-9 probe transmitting 2.5 MHz pulses. The subharmonic imaging presets on this system generate 3 pulse amplitude modulation firings of 4 cycle pulses with a Gaussian windowed binomial filtered square wave with dynamic focusing. Data were acquired at 11 frames per second with a 0.5 MHz bandwidth filter centered around the subharmonic (1.25 MHz). A power optimization sequence, which steps through each available acoustic output power up to 50% was activated and the region of maximal SHAPE sensitivity within the subharmonic growth phase was identified.¹⁸ The selected optimized acoustic power was then used to collect 5 seconds of subharmonic data in triplicate at 0, 26, 52, and 78 mmHg overpressure. Linear regression analyses were used to compare SHAPE data (ie, subharmonic amplitudes) and hydrostatic pressures in GraphPad Prism V9 (San Diego, CA).

Results

Initial monodisperse lipid microbubbles were successfully fabricated with approximate mean diameters of 2.4, 3.3, 3.6, 4.4, and 5.3 μm diameter with corresponding polydispersity index (PDI) of 8.7, 8.5, 7.8, 7.4, and 7.1%, and GSD of 1.09, 1.09, 1.08, 1.08, and 1.07, respectively. These data are shown in Figure 1 with SonoVue (mean diameter = 1.0 μm , PDI = 36.6, GSD = 1.35) provided for comparison. Shelf stability following activation was

also investigated over a 24-hour period in a similar population of 4.0 μm bubbles and demonstrated less than 10% change over time in mode diameter, indicating changes in size resulting from gas diffusion *in vitro* are negligible (Figure 2).

Attenuation curves were generated for each microbubble population shown in Figure 1 and used to determine the corresponding resonance frequency. Attenuation curves of 2.4, 3.3, 3.6, 4.4, and 5.3 μm in diameter monodisperse bubbles and of SonoVue are shown in Figure 3A. Resonance frequencies for the monodisperse bubbles ranged from 2.1 to 6.3 MHz. As expected, monodisperse bubbles showed a much tighter attenuation band relative to the polydisperse commercial agent (approximate -6 dB bandwidths of 1.5 MHz vs. 7 MHz). Figure 3B shows the correlation between monodisperse bubble populations and their resonance frequency ($R^2 > 0.99$). The resonance frequency, as expected, decreases with increasing radius.

Initial experiments with single element transducers were used to confirm the generation of subharmonic signals from the monodisperse microbubbles. Example frequency spectra from a 4 μm diameter population of bubbles are shown in Figure 4. Clear peaks are seen at the driving frequency and the second harmonic (approximately 3.75 and 7.5 MHz, respectively) at all insonation pressures. Occurrence of the subharmonic peak (dotted lines) begins at 150 kPa peak negative pressure. Subharmonic amplitude as a function of acoustic pressure

is also provided in Figure 4, demonstrating nonlinear, S-curve behavior previously described in the literature.^{8,9}

As a proof of concept, the sensitivity of 3.0 and 3.5 μm monodisperse bubbles to hydrostatic pressure were compared to Sonazoid using a commercially available scanner and SHAPE algorithm. Subharmonic signal was visible in the dual imaging mode for all agents (Figure 5; left images). Acoustic output optimization was run for each agent to determine the optimal transmit pressure for SHAPE. Time-intensity curves of the subharmonic amplitude during incremental acoustic output increases (Figure 5; right graphs) demonstrated the nonlinear S-curve behavior previously described in the literature^{8,9} for all agents. However, it was noted that microbubble destruction was observed at lower acoustic outputs (a mechanical index of approximately 0.25) for the monodisperse bubbles relative to Sonazoid (Figure 5; white arrows). Following acoustic output optimization, SHAPE data were collected at 0, 26, 52, and 78 mmHg overpressure (Figure 6). Subharmonic signal from all agents demonstrated an inverse linear relationship with hydrostatic pressure. Sonazoid demonstrated an overall sensitivity of -0.081 dB/mmHg and a correlation of $R^2 = 0.96$. The population of monodisperse 3.0 μm bubbles showed an overall sensitivity of -0.137 dB/mmHg and correlation of $R^2 = 0.96$. The population of monodisperse 3.5 μm bubbles showed an overall sensitivity of -0.168 dB/mmHg and correlation of $R^2 = 0.93$.

Discussion

Noninvasive and accurate measurement of pressure using SHAPE has been demonstrated in a variety of clinical applications.^{10–18} Sonazoid was first shown to be useful for the diagnosis of portal hypertension in canine models and in a pilot, human clinical trial.^{11,13} More recently, these findings were validated as part of a multi-center clinical trial and also shown to be effective for monitoring progression of portal pressures in patients with chronic liver disease.^{14,15,28} In addition, Sonazoid-based SHAPE has been shown to be feasible for the noninvasive measurement of cardiac pressures in both canines and humans.^{10,29} Similar translation has been undertaken using SHAPE with Definity (Lantheus Medical Imaging, N Billerica, MA) for cardiac pressure estimation,¹⁶ and for tracking

changes in interstitial fluid pressure in breast cancers over the course of neoadjuvant chemotherapy.¹⁷ SHAPE using Lumason/SonoVue has also been demonstrated *in vitro*, although a positive linear relationship was observed with hydrostatic pressure up to 75 mmHg switching to an inverse linear relationship above 125 mmHg similar to other agents.³⁰ While results from these studies are encouraging, the sensitivity of SHAPE at lower hydrostatic pressures remains limited. This may be particularly important in lower pressure applications such as differentiating normal patients from patients needing moderate pharmacological intervention for portal hypertension, right heart pressures (2–6 mmHg for the right atrial pressure and 0–8 mmHg diastolic pressure in the right ventricle are considered normal), and monitoring of intracranial pressures (where a difference of 5 mmHg differentiates normal conditions versus those requiring intervention).

Results described in this work show that monodisperse microbubbles specifically designed for SHAPE have the potential to greatly increase sensitivity to hydrostatic pressure compared to relying on polydisperse agents designed for diagnostic imaging. Monodisperse lipid bubbles were shown to be well controlled and stable for up to 24 hours following activation. The resonance frequency of these agents was shown to be well defined and correlating strongly with mean diameter. While these bubbles were found to be less stable at higher acoustic pressures (microbubble destruction was observed in Figure 5 at a mechanical index of approximately 0.25), a strong inverse correlation ($R^2 > 0.93$) was observed, and the sensitivities (-0.14 to -0.17 dB/mmHg) were nearly double the current sensitivity being achieved with a commercial agent. Interestingly, the optimal acoustic output for these agents was found to be higher than the commercial UCA as shown in Figure 5. These findings demonstrate the potential improvements to SHAPE suggested by modeling work predicting the behavior of single or monodisperse bubble populations.^{19–23}

While our results are encouraging, several limitations exist and should be further explored moving forward. Modeling work stresses the importance of matching acoustic parameters to the specific microbubble used to maximize SHAPE sensitivity.¹⁹ This includes matching of resonance frequency (which varies dramatically by size as shown in Figure 3), pulse length, and pulse shape, all of which have been

shown to influence subharmonic and SHAPE behavior.^{11,31} We expect optimization and tailoring of acoustic transmit parameters can be achieved moving forward to further improve the sensitivity of SHAPE. To accommodate inherent variability in future patients, this may require modeling efforts or real-time feedback (similar to what is currently used to optimize acoustic outputs on a patient-by-patient basis¹⁸). A second limitation involves the use of saline at room temperature, due to benchtop setup restrictions. While hematocrit concentration in blood mimicking fluid and in patients with chronic liver disease has been shown to not influence SHAPE,³² temperature may influence diffusion of the gas bubble over time and effect SHAPE measurements. Finally, results to date are based entirely on static conditions *in vitro* with a limited number of sizes. Future work *in vivo* is needed to assess improved sensitivity of these agents under physiologically relevant conditions over a variety of sizes before findings can be fully extrapolated to clinical applications.

In conclusion, the current sensitivity of SHAPE for noninvasive pressure estimation is limited by reliance on clinically approved, polydisperse microbubbles fabricated for diagnostic imaging. This study demonstrates the potential improvements in SHAPE sensitivity using customized, monodisperse microbubbles. Future tailoring of acoustic transmit parameters to specific monodisperse bubbles is expected to further improve these sensitivities and justify further translation toward clinical applications.

References

- Connors AF Jr, Speroff T, Dawson NV, et al. The effectiveness of right heart catheterization in the initial care of critically ill patients. Support investigators. *JAMA* 1996; 276:889–897.
- Shah MR, Hasselblad V, Stevenson LW, et al. Impact of the pulmonary artery catheter in critically ill patients: meta-analysis of randomized clinical trials. *JAMA* 2005; 294:1664–1670.
- Sanyal AJ, Bosch J, Blei A, Arroyo V. Portal hypertension and its complications. *Gastroenterology* 2008; 134:1715–1728.
- Bouakaz A, Frinking PJ, de Jong N, Bom N. Noninvasive measurement of the hydrostatic pressure in a fluid-filled cavity based on the disappearance time of micrometer-sized free gas bubbles. *Ultrasound Med Biol* 1999; 25:1407–1415.
- Fairbank WM Jr, Scully MO. A new noninvasive technique for cardiac pressure measurement: resonant scattering of ultrasound from bubbles. *IEEE Trans Biomed Eng* 1977; 24:107–110.
- Hok B. A new approach to noninvasive manometry: interaction between ultrasound and bubbles. *Med Biol Eng Comput* 1981; 19:35–39.
- Pickering TG, Hall JE, Appel LJ, et al. Recommendations for blood pressure measurement in humans and experimental animals: part 1: blood pressure measurement in humans: a statement for professionals from the subcommittee of professional and public education of the american heart association council on high blood pressure research. *Circulation* 2005; 111:697–716.
- Shi WT, Forsberg F, Raichlen JS, Needleman L, Goldberg BB. Pressure dependence of subharmonic signals from contrast microbubbles. *Ultrasound Med Biol* 1999; 25:275–283.
- Halldorsdottir VG, Dave JK, Leodore LM, et al. Subharmonic contrast microbubble signals for noninvasive pressure estimation under static and dynamic flow conditions. *Ultrason Imaging* 2011; 33:153–164.
- Dave JK, Halldorsdottir VG, Eisenbrey JR, et al. Noninvasive LV pressure estimation using subharmonic emissions from microbubbles. *JACC Cardiovasc Imaging* 2012; 5:87–92.
- Dave JK, Halldorsdottir VG, Eisenbrey JR, et al. Investigating the efficacy of subharmonic aided pressure estimation for portal vein pressures and portal hypertension monitoring. *Ultrasound Med Biol* 2012; 38:1784–1798.
- Halldorsdottir VG, Dave JK, Eisenbrey JR, et al. Subharmonic aided pressure estimation for monitoring interstitial fluid pressure in tumours—in vitro and in vivo proof of concept. *Ultrasonics* 2014; 54:1938–1944.
- Eisenbrey JR, Dave JK, Halldorsdottir VG, et al. Chronic liver disease: noninvasive subharmonic aided pressure estimation of hepatic venous pressure gradient. *Radiology* 2013; 268:581–588.
- Gupta I, Eisenbrey JR, Machado P, et al. Diagnosing portal hypertension with noninvasive subharmonic pressure estimates from a US contrast agent. *Radiology* 2021; 298:104–111.
- Gupta I, Fenkel JM, Eisenbrey JR, Machado P, Stanczak M, Wessner CE, Shaw CM, Miller C, Soulen MC, Wallace K, Forsberg F. A noninvasive ultrasound based technique to identify treatment responders in patients with portal hypertension. *Acad Radiol* 2020; S1076-633230675-9.
- Dave JR, Kulkarni SV, Pangaonkar PP, et al. Non-invasive intracardiac pressure measurements using subharmonic-aided pressure estimation: proof of concepts in humans. *Ultrasound Med Biol* 2017; 43:2718–2724.
- Nam K, Eisenbrey JR, Stanczak M, et al. Monitoring neoadjuvant chemotherapy of breast cancer by using 3D subharmonic aided pressure estimation and imaging with US contrast agents: preliminary experience. *Radiology* 2017; 285:53–62.
- Forsberg F, Gupta I, Machado P, et al. Contrast-enhanced subharmonic aided pressure estimation (SHAPE) using ultrasound imaging with a

- focus on identifying portal hypertension. *J Vis Exp* 2020. <https://doi.org/10.3791/62050>
19. Katiyar A, Sarkar K, Forsberg F. Modeling subharmonic response from contrast microbubbles as a function of ambient static pressure. *J Acoust Soc Am* 2011; 129:2325–2335.
 20. Andersen KS, Jensen JA. Ambient pressure sensitivity of microbubbles investigated through a parameter study. *J Acoust Soc Am* 2009; 126:3350–3358.
 21. Andersen KS, Jensen JA. Impact of acoustic pressure on ambient pressure estimation using ultrasound contrast agent. *Ultrasonics* 2010; 50:294–299.
 22. Katiyar A, Sarkar K. Excitation threshold for subharmonic generation from contrast microbubbles. *J Acoust Soc Am* 2011; 130: 3137–3147.
 23. Katiyar A, Sarkar K. Effects of encapsulation damping on the excitation threshold for subharmonic generation from contrast microbubbles. *J Acoust Soc Am* 2012; 132:3576–3585.
 24. Huh D, Bahnq JH, Ling Y, et al. Gravity-driven microfluidic particle sorting device with hydrodynamic separation amplification. *Anal Chem* 2007; 79:1369–1376.
 25. Hettiarachchi K, Talu E, Longo ML, Dayton PA, Lee AP. On-chip generation of microbubbles as a practical technology for manufacturing contrast agents for ultrasonic imaging. *Lab Chip* 2007; 7:463–468.
 26. Chen JL, Dhanaliwala AH, Dixon AJ, Klivanov AL, Hossack JA. Synthesis and characterization of transiently stable albumin-coated microbubbles via a flow-focusing microfluidic device. *Ultrasound Med Biol* 2014; 40:400–409.
 27. de Jong N, Hoff L, Skotland T, Bom N. Absorption and scatter of encapsulated gas filled microspheres: theoretical considerations and some measurements. *Ultrasonics* 1992; 30:95–103.
 28. Machado P, Gupta I, Gummadi S, et al. Hepatic vein contrast-enhanced ultrasound subharmonic imaging signal as a screening test for portal hypertension. *Dig Dis Sci* 2021. <https://doi.org/10.1007/s10620-020-06790-6>.
 29. Esposito C, Dickie K, Forsberg F, Dave JK. Developing an interface and investigating optimal parameters for real-time intracardiac subharmonic-aided pressure estimation. *IEEE Trans Ultrason Ferroelectr Freq Control* 2021; 68:579–585.
 30. Nio AQX, Faraci A, Christensen-Jeffries K, et al. Optimal control of SonoVue microbubbles to estimate hydrostatic pressure. *IEEE Trans Ultrason Ferroelectr Freq Control* 2020; 67:557–567.
 31. Gupta I, Eisenbrey J, Stanczak M, et al. Effect of pulse shaping on subharmonic aided pressure estimation in vitro and in vivo. *J Ultrasound Med* 2017; 36:3–11.
 32. Gupta I, Eisenbrey JR, Machado P, Stanczak M, Wallace K, Forsberg F. On factors affecting subharmonic-aided pressure estimation (SHAPE). *Ultrason Imaging* 2019; 41:35–48.